Role of the spinal canal compliance in regulating posture-related cerebrospinal fluid hydrodynamics in humans

Noam Alperin, PhD,[1,2*] Ritambhar Burman, BE,[1,2] and Sang H. Lee, MS[1]

Mechanical compliance of a compartment is defined by the change in its volume with respect to a change in the inside pressure. The compliance of the spinal canal regulates the intracranial pressure (ICP) under postural changes. Understanding how gravity affects ICP is beneficial for poorly understood cerebrospinal fluid (CSF)-related disorders. The aim of this study was to evaluate postural effects on cranial hemo- and hydrodynamics. This was a prospective study, which included 10 healthy volunteers (three males, seven females, mean ± standard deviation age: 29 ± 7 years). Cine gradient-echo phase-contrast sequence acquired at 0.5 T, "GE double-doughnut" scanner was used. Spinal contribution to overall craniospinal compliance (CSC), craniospinal CSF stroke volume (SV), magnetic resonance (MR)-derived ICP (MR-ICP), and total cerebral blood flow (TCBF) were measured in supine and upright postures using automated blood and CSF flows quantification. Statistical tests performed were two-sided Student's *t*-test, Cohen's *d*, and Pearson correlation coefficient. MR-ICP and the craniospinal CSF SV were significantly correlated with the spinal contribution to the overall CSC ($r = 0.83$, $p < 0.05$) and ($r = 0.62$, $p < 0.05$), respectively. Cranial contribution to CSC increased from 44.5% ± 16% in supine to 74.9% ± 8.4% in upright posture. The average MR-ICP dropped from 9.9 ± 3.4 mmHg in supine to −3.5 ± 1.5 mmHg. The CSF SV was over 2.5 times higher in the supine position (0.55 ± 0.14 ml) than in the upright position (0.21 ± 0.13 ml). In contrast, TCBF was slightly higher in the supine posture (822 ± 152 ml/min) than in the upright posture (761 ± 139 ml/min), although not statistically significant ($p = 0.16$). The spinal-canal compliance contribution to CSC is larger than the cranial contribution in the supine posture and smaller in the upright posture. Thereby, the spinal canal plays a role in modulating ICP upon postural changes. The lower pressure craniospinal CSF system was more affected by postural changes than the higher-pressure cerebral vascular system. Craniospinal hydrodynamics is affected by gravity and is likely to be altered by its absence in space.
Level of Evidence: 4
Technical Efficacy Stage: 2

J. MAGN. RESON. IMAGING 2021.

Introduction

The craniospinal cerebrospinal fluid (CSF) compartment in humans extends from the top of the brain to the bottom of the sacrum. Because of gravity, body posture influences craniospinal hydrodynamics, including cranial and spinal CSF volumes, craniospinal CSF stroke volume (SV), cranial and spinal compliances, and intracranial pressure (ICP).[1,2] Quantitative characterization of the craniospinal system hydrodynamics under different postures may help in the diagnosis and treatment of CSF-related disorders. For example, it is likely to improve CSF shunting performance as recent observation links high failure rate of shunting to overdrainage, primarily in the upright posture.[3]

Mechanical compliance determines the relation between changes in CSF volume and pressure. Each of the two subcompartments has a different compliance; therefore, both sub-compartments regulate the craniospinal hydrodynamics during changes in posture. Currently used invasive methods to measure craniospinal compliance (CSC) do not provide information on the individual sub-compartments; therefore, we developed and applied methodology to quantify the cranial and spinal canal contribution to the overall CSC in the supine and the upright postures.

Data available on the CSC distribution are not only limited but is also inconsistent with conflicting information regarding which sub-compartment provides the majority of

View this article online at wileyonlinelibrary.com. DOI: 10.1002/jmri.27505

Received Sep 13, 2020, Accepted for publication Dec 28, 2020.

*Address reprint requests to: Noam Alperin, 1150 NW 14th St #713, Miami, FL 33136, USA. E-mail: nalperin@med.miami.edu

From the [1]Radiology Department, University of Miami, Miami, Florida, USA; and [2]Biomedical Engineering Department, University of Miami, Miami, Florida, USA

the CSC.[2,4–8] Lofgren and Zwetnow presented a constant-rate infusion method in dogs to measure the overall CSC.[5] They applied a spinal block at C1 level to obtain measurement of the compliances of the individual compartments and reported that cranial compliance was smaller than spinal compliance.[6] Magnaes[2] used a similar infusion-based method in supine patients with CSF blockage at the upper cervical level and reported that only 37% of the total compliance came from the cranium. A constant pressure infusion test,[8] in conjunction with magnetic resonance imaging (MRI) measurements of blood and CSF flows into and out of the cranium, were used to compute a pressure-volume index, which is a measure of compliance, in the supine posture in aged healthy subjects. The measurement of CSF flow at the upper cervical level provided a way to estimate the compliances of the two sub-compartments individually. The study reported larger cranial contribution (65%) than the spinal contribution (35%). Follow-up work by Tain et al.[7] demonstrated that when the pulsatile cerebral venous drainage was accounted for in the measurement of the intracranial volume change during the cardiac cycle, the spinal canal provided the majority of the overall compliance.

Tain et al.[7] implemented a noninvasive MRI-based method that, in conjunction with a lumped-parameter subject-specific model, provided the relative contributions of the cranial and spinal compartments to the overall CSC in healthy and in idiopathic intracranial hypertension patients. A modified implementation of the method that constrained the solutions to stable and positive values was applied to study the effect of age on the CSC.[4]

The aim of this study is to measure the CSC distribution in upright and supine postures, to determine relationships between the compliance contributions of each sub-compartment and ICP, and to assess the impact of gravity on the craniospinal hydrodynamics and the cerebral blood flow.

Materials and Methods

Subjects and Imaging

The imaging protocol was approved by the institutional review board and written informed consent was obtained from all subjects. Inclusion and exclusion criteria were healthy subjects, age 18 and above, and without known history of neurological or neurosurgical problems. Imaging was performed in upright and supine positions in a Signa SP/i 0.5 T vertical gap MR scanner (GE Medical Systems, Milwaukee, MN, USA) as described in a previous publication.[1]

Cine phase-contrast gradient-echo sequence was used separately to obtain high- and low-velocity-encoding (VENC) images for measurements of the blood and CSF flows to and from the cranium, respectively, as previously described.[1] Briefly, the high- and

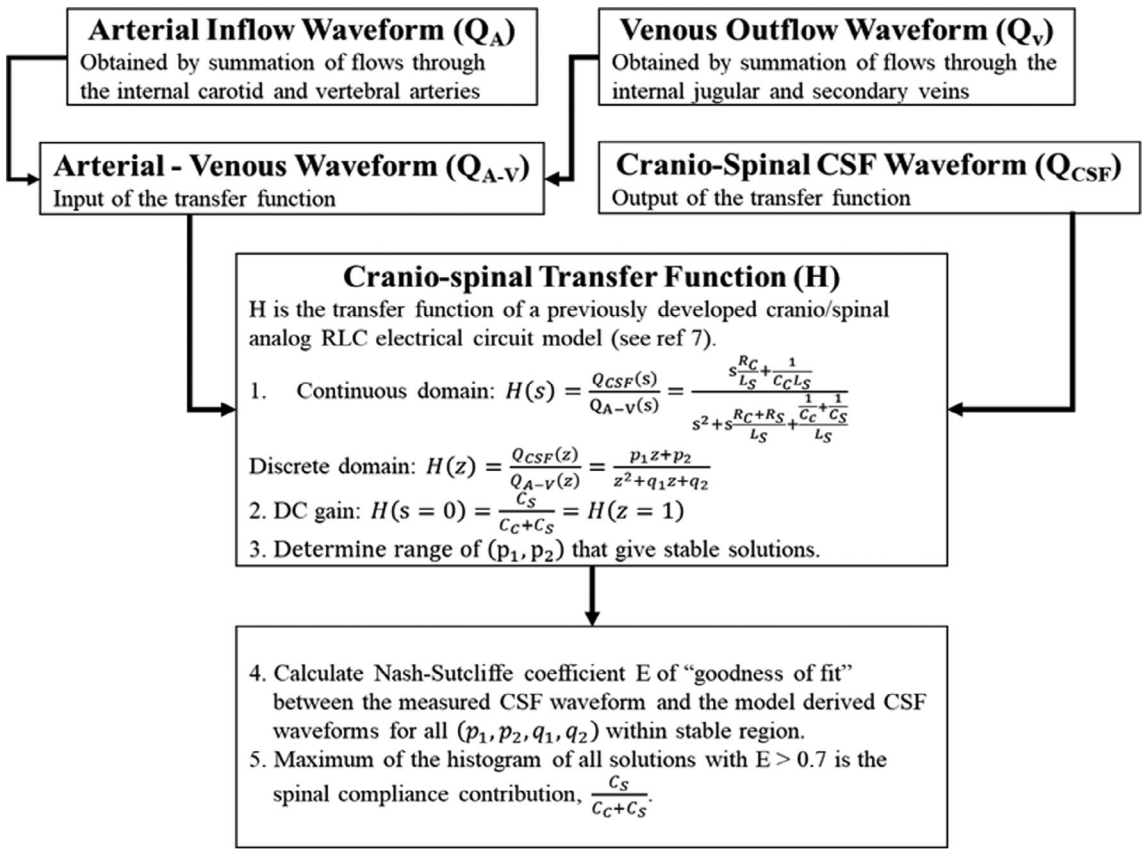

Figure 1: Summary flow chart of the processing pipeline for the derivation of the spinal and cranial contributions to cranio-spinal compliance

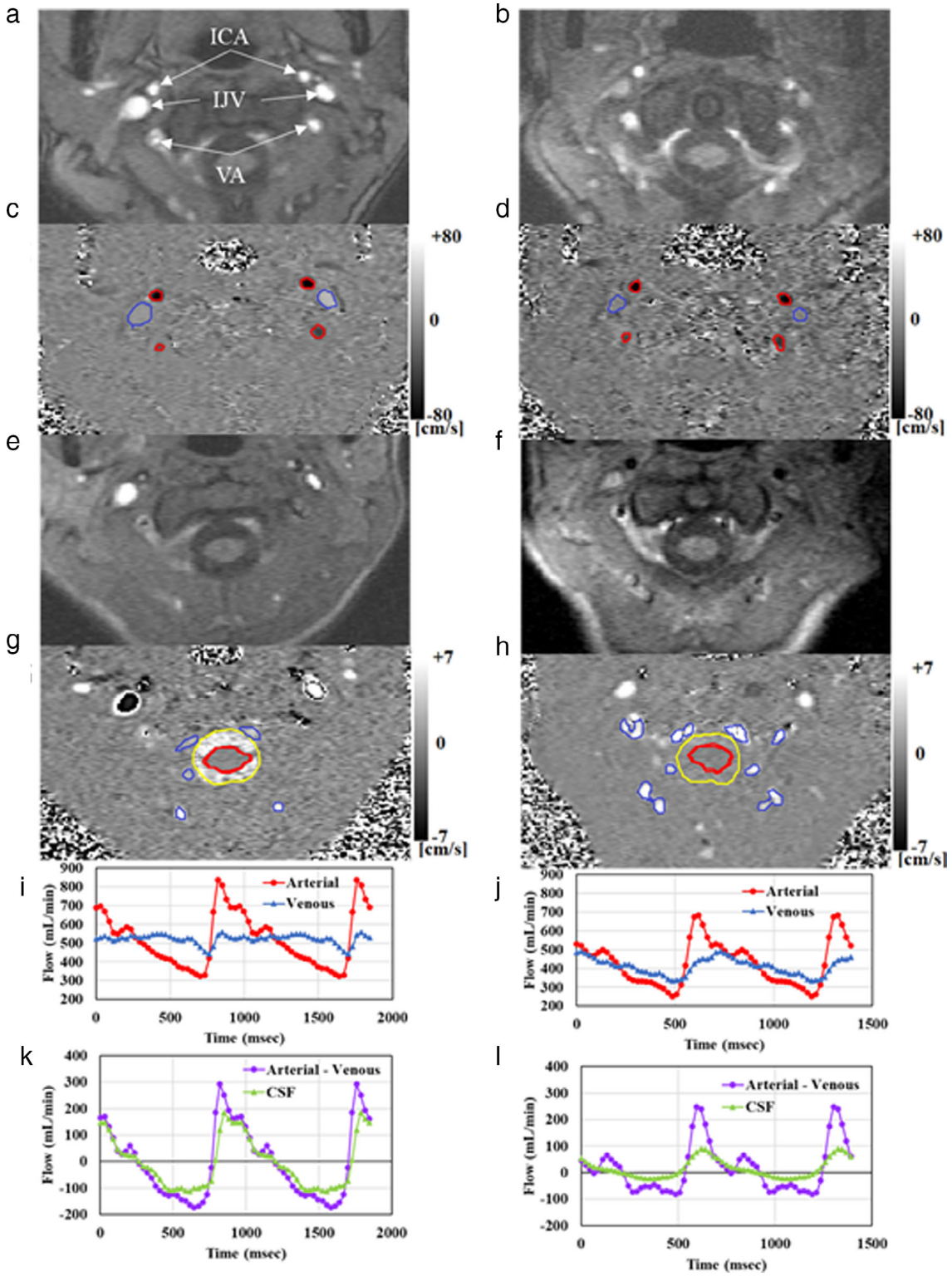

Figure 2: Examples of the blood and cerebrospinal fluid (CSF) volumetric flow rate measurements from MR scans for the supine (left column) and upright (right column) postures. A-B: Anatomical gradient echo images corresponding to high VENC blood flow scan. C-D: The high velocity-encoded phase contrast images used for measurements of arterial inflow (red lumens) and venous outflow (blue lumens). White pixels (positive values) represent velocity in the cranio-caudal direction, and black pixels (negative values) represent flow in the opposite direction. E-F: Anatomical gradient echo images corresponding to low VENC CSF flow scan. G-H: The velocity-encoded phase contrast images used for measurements of CSF flow (yellow lumen) with the cord in the middle (red lumen). Note additional venous pathways (blue lumens) seen in the upright posture, are not seen in the supine scan. I-J: Derived arterial and venous blood volumetric flow rate waveforms. Note the similarity in the flow pattern between the arterial waveforms and the lack of it in the venous waveforms. K-L: The CSF flow waveforms (green) superimposed on the arterio-venous flow waveforms (purple). Note how closely the CSF waveform follows the A-V waveform in the supine posture, indicating a low cranial compliance in the supine posture compared to the upright posture state where the CSF waveform does not follow the A-V as closely

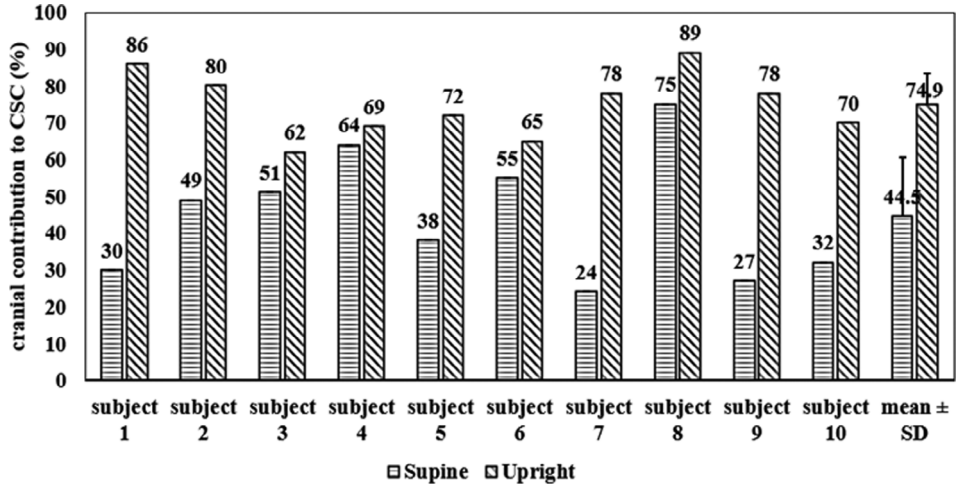

Figure 3: Cranial contribution to total cranio-spinal compliance (CSC) in supine and upright postures for all subjects followed by the global mean ± standard deviation

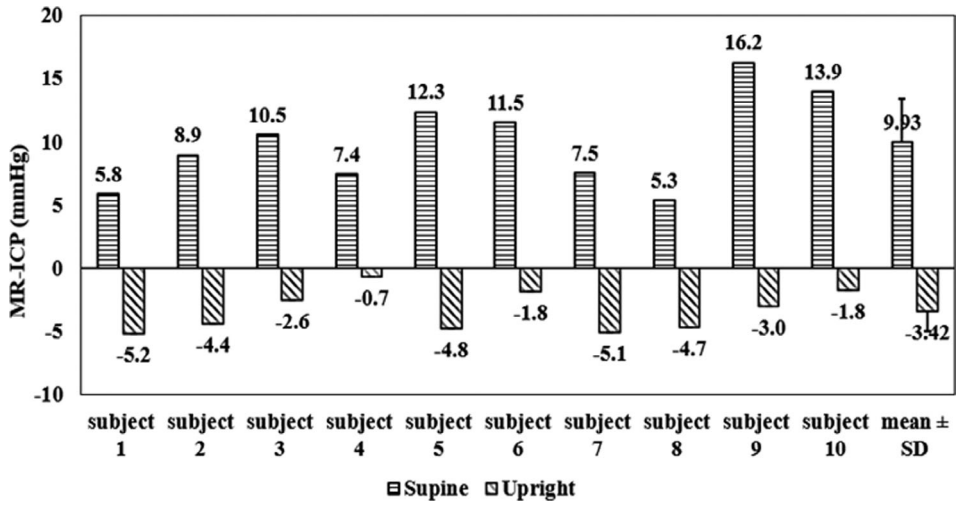

Figure 4: magnetic resonance (MR)-derived intracranial pressure (MR-ICP) measurements for both supine and upright postures for all subjects, followed by the global mean ± standard deviation. Subjects are in the same order as shown in Figure 3

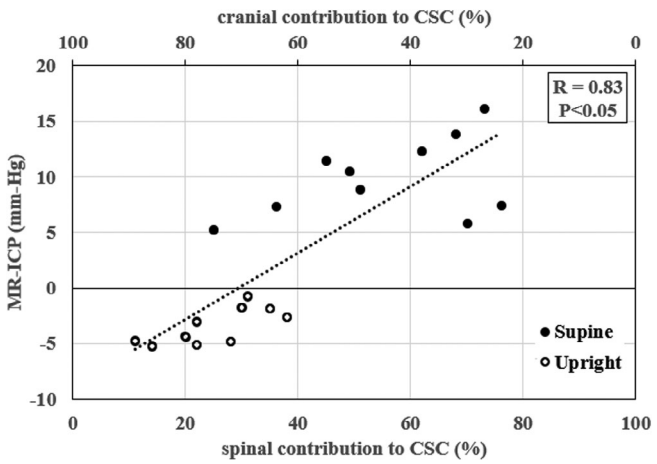

Figure 5: Linear regression (dotted line) of magnetic resonance (MR)-derived intracranial pressure (MR-ICP) and spinal contribution to total cranio-spinal compliance (CSC) when both supine (filled dots) and upright posture data (hollow dots) were combined

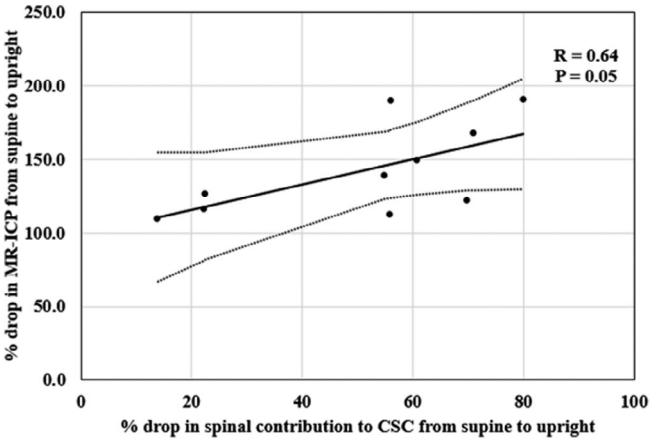

Figure 6: Linear regression (solid line) between percentage drop in magnetic resonance (MR)-derived intracranial pressure (MR-ICP) and percentage drop in spinal contribution to cranio-spinal compliance (CSC) following a change from supine to upright posture. The dotted outer lines indicate the 95% confidence interval

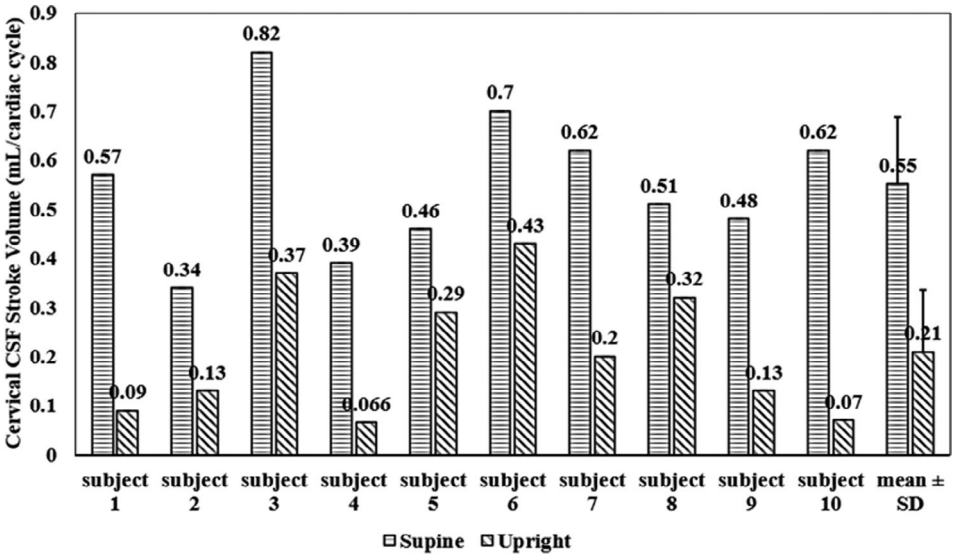

Figure 7: Cervical cerebrospinal fluid (CSF) stroke volume in the supine and upright postures for all subjects, followed by the global mean ± standard deviation. Subjects are in the same order as in Figure 3

low-velocity encodings were 80 and 7–9 cm/s, respectively. In-plane resolution was 0.62×0.62 mm^2 with a slice thickness of 8 mm. The imaging plane for blood flow was placed at the dens level perpendicular to the internal carotid and vertebral arteries and for imaging the CSF at mid-C2 level.

Image Processing

An automated vessel and CSF lumen segmentation for the calculation of flow rates was performed using the pulsatility-based segmentation (PUBS) method.[9] The PUBS method[9] utilizes an automated algorithm to segment lumens with nonsteady flow. The method utilizes temporal information from the entire image series to differentiate between lumen and surrounding pixels. The PUBS method demonstrated high inter- and intraclass correlation coefficient (above 0.9 and 0.96, respectively) for the measurements of blood and CSF volumetric flows rates.[10]

Derivation of the Hemodynamic Parameters

Total arterial flow to the brain, or total cerebral blood flow (TCBF), was obtained by summing the volumetric flow rates through the internal carotid and vertebral arteries. Venous outflow was obtained by summing the flow through the internal jugular veins and through the epidural, vertebral, and deep cerebral veins, when present. Background correction to correct for phase biases was performed for all lumens. Cervical CSF SV was calculated as the volume of CSF that moves between the cranium and spinal canal with each cardiac cycle.

MRI-Based Derivation of the ICP

The derivation of ICP has been described previously.[11] Briefly, dV, the intracranial volume change (ICVC) during the cardiac cycle, was calculated from the momentary difference between blood and CSF volumes entering and leaving the cranium. The resulting change in pressure, dP, is proportional to the amplitude of the CSF pressure gradient waveform obtained using Navier–Stokes relationship.[12] The cranial elastance (dP/dV) was derived from the maximum changes in pressure and intracranial fluids' volume during the cardiac cycle. The MR-derived ICP (MR-ICP) was then determined based on the linear relationship between the elastance and ICP.[13] In the upright posture, MR-ICP was adjusted to account for the hydrostatic pressure between the skull base, where the CSF flow is measured, and the middle of the skull, the reference point for the ICP.[14]

Derivation of the Cranial and Spinal Contributions to the Overall CSC Compliance

The derivation of the relative contributions of the cranium and spinal canal to the overall CSC has been described previously.[4] The measured transcranial blood and CSF flows (the same data used to calculate the MR-ICP) were used in an analogous lumped-parameter electrical model which takes into account the resistances and compliances of the cranium and spinal canal, respectively, and the inertia of the CSF flow in the upper spinal canal. The arterial minus the venous flow was considered the driving force and the input of the model, and the CSF flow as the output. A constrained least square

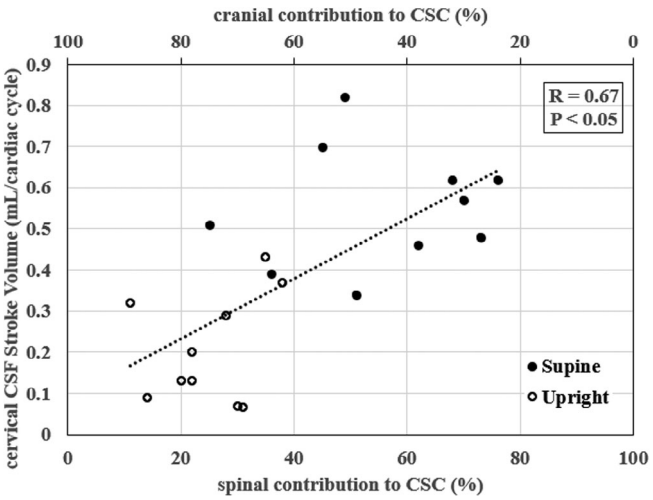

Figure 8: Linear regression (dotted line) of cerebrospinal fluid (CSF) stroke volume and spinal contribution to cranio-spinal compliance (CSC) when both supine (filled dots) and upright (hollow dots) posture data were combined

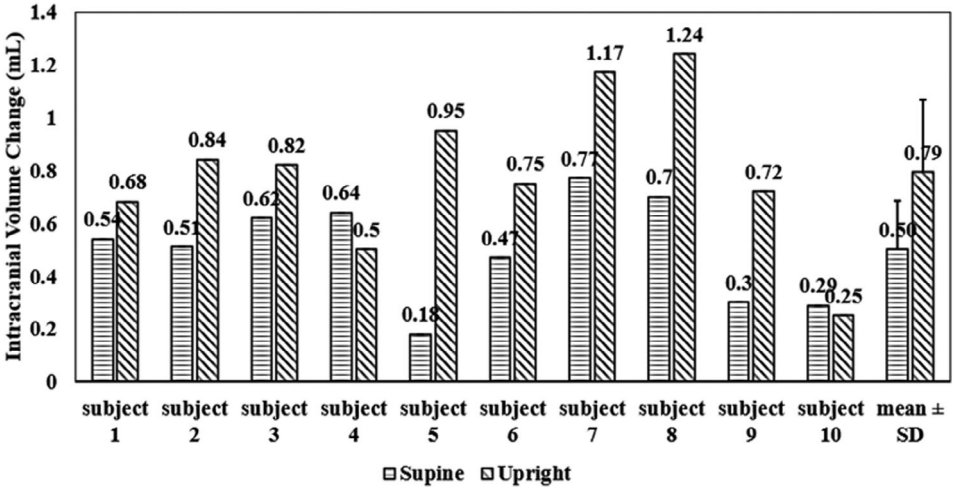

Figure 9: The maximum intracranial volume change (ICVC) during a cardiac cycle in the supine and upright positions for all subjects, followed by the global mean ± standard deviation. Subjects are in the same order as in Figure 3

search was used to estimate the model transfer function and derive the relative contributions of the cranial and spinal canal compliances to the total CSC. A schematic summary of the global processing pipeline showing the different steps for processing of the cranial and spinal canal contributions to the overall CSC is shown in Figure 1. In addition, percent drop in MR-ICP and spinal contribution to CSC were calculated for a change in posture for supine to upright.

Statistical Analysis

The Pearson correlation coefficient was used to obtain a linear regression of the relationships between the cranial and spinal contributions to the total CSC, and the MR-ICP, and the cervical CSF SV for the upright posture, supine posture, and both postures combined. Pearson correlation coefficient was used to obtain a linear regression of the relationship between the percent drop in MR-ICP and percent drop in spinal contribution to CSC on changing from supine to upright posture. A Shapiro–Wilks test was performed to check the normality of pressure distributions in both the postures, with $p > 0.05$ indicating a normal distribution. Two-sided Student's *t*-test was used throughout the analysis, and $p < 0.05$ was considered statistically significant. Paired two-sided Student's *t*-test along with Cohen's *d* effect size were calculated when comparing spinal and cranial contribution to CSC, MR-ICP, TCBF, ICVC, cervical CSF SV between upright and supine postures. A Shapiro–Wilks test was performed using the SPSS software, v. 22 (IBM, Armonk, NY). All other statistical calculations were performed in Excel (Windows v. 2016, Redmond, WA). All figures were plotted in Excel (Windows v. 2016, Redmond, WA).

Results

Ten healthy volunteers (three males and seven females, mean ± SD age: 29 ± 7 years), were included in the study.[1] An example of high- and low-velocity-encoding phase contrast images from a subject in supine (left) and upright (right) postures, and the corresponding arterial, venous, and CSF

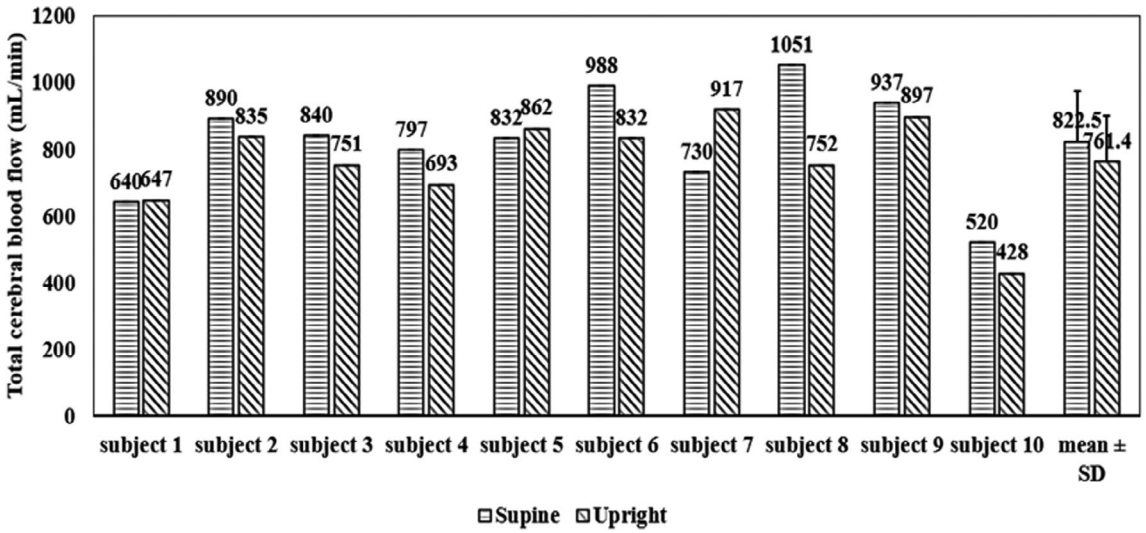

Figure 10: Total cerebral blood flow (TCBF) in the supine and upright postures for all subjects, followed by the global mean ± standard deviation. Subjects are in the same order as in Figure 3

flows' waveforms are shown in Figure 2. The cranial and spinal contributions to total CSC for each subject and the mean and SD are shown in Figure 3. Average cranial contribution to total CSC was significantly lower in the supine posture than in the upright posture (44.5% ± 16% vs. 74.9% ± 8.4%, respectively, $p < 0.05$, Cohen's $d = 2.36$). MR-ICP in the upright (accounting for the hydrostatic pressure) and the supine postures are shown in Figure 4. The average MR-ICP was significantly higher in the supine position than in the upright posture (9.9 ± 3.4 mmHg vs. −3.5 ± 1.5 mmHg, respectively, $p < 0.05$ Cohen's $d = 5.06$). A significant positive correlation between MR-ICP and the spinal contribution to total CSC ($r = 0.83$, $p < 0.05$) was observed when both supine and upright posture data were combined (Figure 5). Individually, there was a significant positive correlation ($r = 0.72$, $p < 0.05$) in the upright posture but not in the supine posture ($r = 0.43$, $p = 0.2$). A positive but not significant correlation between percent drop in MR-ICP and percent drop in spinal contribution to CSC was observed in changing posture from supine to upright ($r = 0.64$, $p = 0.05$), with seven out of 10 points lying within the 95% confidence band for regression (Figure 6).

The craniospinal CSF SVs for each subject measured in the supine and the upright postures and the mean and SD are shown in Figure 7. On average, SV was over 2.5 times higher in the supine position than in the upright position (0.55 ± 0.14 ml/cardiac cycle vs. 0.21 ± 0.13 ml/cardiac cycle, respectively, $p < 0.05$, Cohen's $d = 2.58$). Linear regression between the CSF SV and the spinal contribution to total CSC (Figure 8) demonstrated a significant positive correlation ($r = 0.62$, $p < 0.05$). Individually, the regressions did not achieve significance for either posture ($r = 0.12$, $p = 0.73$ in supine; $r = 0.32$, $p = 0.36$ in upright). On average, maximum ICVC during a cardiac cycle (Figure 9) was significantly higher in the upright posture (approximately 1.6 times) than in the supine posture (0.5 ± 0.18 ml vs. 0.79 ± 0.28 ml, respectively, $p < 0.05$ Cohen's $d = 1.23$). On average, TCBF (Figure 10) was higher in the supine posture than in the upright posture by about 9%; however, this difference was not significant (822 ± 152 ml/min vs. 761 ± 139 ml/min, $p = 0.16$, Cohen's $d = 0.42$).

Discussion

Our results demonstrate the effect of body posture on the relative contributions of the cranium and spinal canal to the overall CSC and how these changes affect the overall craniospinal hydrodynamics and the total cerebral blood flow. We found that the spinal canal contributed slightly more than the cranial to the overall CSC in the supine posture and that the cranium provided the majority of the compliance in the upright posture. The relatively larger spinal compliance in the supine posture might be related to the fact that dura in the spinal canal is less confined by the vertebra than it is in the cranium, especially in the lumbar region.[15] In contrast, TCBF was similar or only slightly reduced in the upright posture.

The larger spinal contribution to the CSC enables a shift of CSF volume from the cranium to the spinal canal upon changing from supine to upright postures, and a reversal shift upon return to supine posture. The positive correlation between the spinal contribution to total CSC and MR-ICP confirms the role of the spinal canal compliance in modulating ICP. In the lack of gravity, the CSF shifts to equalize the pressures in the cranium and the spinal canal, therefore in space, the craniospinal distribution of the CSF is more similar to its distribution in supine than in the upright posture. As a result, astronauts in space experience on average, a higher cranial CSF volume compared to while on Earth. This is consistent with reports that severity of ocular deformations in astronauts, also known as spaceflight-induced neuro-ocular syndrome, were correlated with pre-to-post flight increase in cranial and orbital CSF volumes following long duration spaceflights.[16,17] A posture of −6° head down tilt (HDT) is widely used by NASA researchers to simulate the condition of microgravity on Earth.[18] The choice of −6° HDT is based on vascular considerations that do not apply to the CSF system.[18] A −6° HDT posture on Earth causes a shift of CSF from the spinal canal to the cranium and that would not result in the same pressure throughout the craniospinal compartment.

Our findings that the average cranial contribution to the CSC in the supine posture was 44% and in the upright posture was 75% are in agreement with the only measurements obtained in humans. Magnaes[2] used infusion in a patient with a cervical block. He found that the cranial compartment contributed 37% and 66% of the total CSC in the supine and upright postures, respectively. The mean cranial contribution of 44% in the supine posture is also in agreement with a previous report of 40% contribution in the supine posture in subjects of similar age.[4]

In the upright posture, gravity pulls the CSF caudally from the cranium to the lower spinal canal, where the majority of the CSC resides.[15] As shown by Marmarou et al., as the volume of a compartment increases, the pressure increases exponentially and compliance decreases inversely with the pressure,[13] explaining the reduced spinal canal compliance contribution to CSC in the upright posture. An increased cranial compliance in the upright posture is consistent with the significant increase in the average maximal ICVC during the cardiac cycle, as a larger compliance allows for a larger volume change for a given increase in pressure.

The trend toward increased cranial contribution to CSC in the upright posture compared to supine is consistent with work by Gehlen et al.,[19] who used a lumped-parameter model that assumed 65% contribution to CSC coming from

the cranium in the supine posture, which then increased to 90% in the upright posture. In the upright posture, there is a large hydrostatic pressure difference between the top of the cranium and the bottom of the spinal canal. The shift of CSF from the cranium to the spinal canal due to gravity decreases the amount of CSF in the cranium. Therefore, the ICP values become low or even slightly negative at the center of the cranium[14] and significantly higher at the lumber regions due to the added hydrostatic pressure.

In the supine posture, where the differential hydrostatic effects on the cranium and spinal canal are minimal, the individual compliances of the cranium and spinal canal dominate the re-distribution of the CSF and, thereby, the change in ICP. This was further demonstrated by the significant positive correlation between ICP and spinal contribution to the total CSC. A larger spinal contribution indicates reduced cranial contribution and, thus, higher ICP. The importance of ICP regulation by the spinal canal is further demonstrated by the trend toward positive correlation between the percentage drop in MR-ICP and the percentage drop in spinal contribution to CSC when changing from supine to upright posture.

The craniospinal CSF SV was positively correlated with the spinal contribution to CSC, as increased spinal compliance allows a larger volume of CSF to enter the spinal canal during the systolic increase in ICP. The average CSF SV in the supine posture was indeed much higher than in the upright posture. These findings may explain the known fact that removal of toxins from the brain is more efficient during sleep[20] when the body is typically in a supine posture. A larger amount of CSF movement between the cranium and the spinal canal increases mixture of the cranial and spinal CSF. Additionally, there seems to be a large inter-individual variability in the magnitudes of the CSF SV and the ICVC among the healthy individual. This can be attributed to inter-individual variability in the venous outflow pattern. Unlike the arterial system, the venous anatomy and functions are highly variable, even among healthy individuals, and measures that depend on venous outflow, for example, CSF SV, ICVC, and even ICP can vary among individuals.

In contrast to the hydrodynamic parameters, for example, CSF SV, ICVC, CSC contribution, and MR-ICP, which are strongly affected by gravity, we found that the average arterial volumetric blood flow to the brain was similar or only slightly reduced in the upright posture. This is because the arterial system operates at a much higher pressure (around 100 mmHg) than the CSF system (around −5 to 15 mmHg), and thus, it is less affected by the changes in hydrostatic pressure.

Limitations

Among the limitations of this study is the small number of subjects which limits the power to identify significant correlations within the individual postural states. A limitation of the methodology is the fact that it provides the relative contribution of each sub-compartment but not the absolute compliances. Measurements of the CSF volume in each sub-compartment would have provided the means to calculate the absolute compliances, but volumetric CSF measurements were not available. Finally, the study was not validated using alternative methods. This is because there are currently no other noninvasive methods to measure the individual compliance contributions of the cranium or the spinal canal. Regardless of these limitations, we achieved the aim of the study to demonstrate the feasibility of the methodology to measure the contributions of each sub-compartment to the overall CSC under different states and describe their associations with other hydrodynamic measures.

Conclusion

Our study elucidated the interplay between the spinal contribution to the CSC and the CSF hydrodynamics. The correlation between the spinal contribution to the overall CSC with MR-ICP in both supine and upright postures combined, and the trend for correlation between the percentage drop in MR-ICP and the percentage drop in spinal contribution to CSC point to the role of the spinal canal compliance contribution to the regulation of ICP at the different body postures. The demonstrated methodology could potentially contribute to poorly understood CSF disorders. Characterization of the craniospinal hydrodynamics under postural changes is analogous to a stress test of the CSF system where impaired function can show up only under postural changes (e.g., CSF shunt malfunction).

References

1. Alperin N, Lee SH, Sivaramakrishnan A, Hushek SG. Quantifying the effect of posture on intracranial physiology in humans by MRI flow studies. J Magn Reson Imaging. 2005;22(5):591–6.
2. Magnaes B. Clinical studies of cranial and spinal compliance and the craniospinal flow of cerebrospinal fluid. Br J Neurosurg. 1989;3(6): 659–68.
3. Kraemer MR, Koueik J, Rebsamen S, Hsu DA, Salamat MS, Luo S, et al. Overdrainage-related ependymal bands: a postulated cause of proximal shunt obstruction. J Neurosurg Pediatr. 2018;22(5):567–77.
4. Burman R, Alperin N, Lee SH, Ertl-Wagner B. Patient-specific craniospinal compliance distribution using lumped-parameter model: its relation with ICP over a wide age range. Fluids Barriers CNS. 2018;15 (1):29.
5. Lofgren J, von Essen C, Zwetnow NN. The pressure-volume curve of the cerebrospinal fluid space in dogs. Acta Neurol Scand. 1973;49(5): 557–74.
6. Lofgren J, Zwetnow NN. Cranial and spinal components of the cerebrospinal fluid pressure-volume curve. Acta Neurol Scand. 1973;49(5): 575–85.
7. Tain RW, Bagci AM, Lam BL, Sklar EM, Ertl-Wagner B, Alperin N. Determination of cranio-spinal canal compliance distribution by MRI: methodology and early application in idiopathic intracranial hypertension. J Magn Reson Imaging. 2011;34(6):1397–404.

8. Wahlin A, Ambarki K, Birgander R, Alperin N, Malm J, Eklund A. Assessment of craniospinal pressure-volume indices. AJNR Am J Neuroradiol. 2010;31(9):1645–50.

9. Alperin N, Lee SH. PUBS: pulsatility-based segmentation of lumens conducting non-steady flow. Magn Reson Med. 2003;49(5):934–44.

10. Koerte I, Haberl C, Schmidt M, Pomschar A, Lee S, Rapp P, et al. Inter- and intra-rater reliability of blood and cerebrospinal fluid flow quantification by phase-contrast MRI. J Magn Reson Imaging. 2013;38(3): 655–62.

11. Alperin NJ, Lee SH, Loth F, Raksin PB, Lichtor T. MR-intracranial pressure (ICP): a method to measure intracranial elastance and pressure noninvasively by means of MR imaging: baboon and human study. Radiology. 2000;217(3):877–85.

12. Loth F, Yardimci MA, Alperin N. Hydrodynamic modeling of cerebrospinal fluid motion within the spinal cavity. J Biomech Eng. 2001;123 (1):71–9.

13. Marmarou A, Shulman K, LaMorgese J. Compartmental analysis of compliance and outflow resistance of the cerebrospinal fluid system. J Neurosurg. 1975;43(5):523–34.

14. Alperin N, Lee SH, Bagci AM. MRI measurements of intracranial pressure in the upright posture: the effect of the hydrostatic pressure gradient. J Magn Reson Imaging. 2015;42(4):1158–63.

15. Alperin N, Bagci AM, Lee SH, Lam BL. Automated quantitation of spinal CSF volume and measurement of craniospinal CSF redistribution following lumbar withdrawal in idiopathic intracranial hypertension. AJNR Am J Neuroradiol. 2016;37(10):1957–63.

16. Alperin N, Bagci AM. Spaceflight-induced visual impairment and globe deformations in astronauts are linked to orbital cerebrospinal fluid volume increase. Acta Neurochir Suppl. 2018;126:215–9.

17. Alperin N, Bagci AM, Oliu CJ, Lee SH, Lam BL. Role of cerebrospinal fluid in spaceflight-induced ocular changes and visual impairment in astronaut. Radiology. 2017;285(3):1063.

18. Hargens AR, Vico L. Long-duration bed rest as an analog to microgravity. J Appl Physiol (1985). 2016;120(8):891–903.

19. Gehlen M, Kurtcuoglu V, Schmid Daners M. Is posture-related craniospinal compliance shift caused by jugular vein collapse? A theoretical analysis. Fluids Barriers CNS. 2017;14(1):5.

20. Xie L, Kang H, Xu Q, Chen MJ, Liao Y, Thiyagarajan M, et al. Sleep drives metabolite clearance from the adult brain. Science. 2013;342 (6156):373–7.